PERGAMON

International Journal of Solids and Structures 37 (2000) 4509–4525

INTERNATIONAL JOURNAL OF SOLIDS and STRUCTURES

www.elsevier.com/locate/ijsolstr

Buckling of thin cylindrical shells under axial compression

P. Mandal [1], C.R. Calladine*

Department of Engineering, University of Cambridge, Cambridge, CB2 1PZ, UK

Received 29 June 1998; in revised form 25 January 1999

Abstract

Simple experiments on self-weight buckling of thin, open-top, fixed-base, small-scale silicone rubber cylindrical shells are presented in this article. The buckling heights were found to be proportional to thickness raised to the power of approximately 1.5, compared to 1.0 as in the classical theory. A non-linear finite-element analysis of self-weight buckling showed that there is a 'post-buckling plateau' load corresponding to the experimental buckling loads. Moreover, the results of the present experiments showed very little 'scatter' in the buckling heights, compared to the large scatter in the experimental data from the literature on the buckling of thin cylindrical shells under axial compressive load (which also have buckling stress proportional to thickness raised to the power of approximately 1.5), although there were measurable imperfections in terms of thickness variations. These observations somehow defy the accepted hypothesis of 'imperfection-sensitivity' in shell buckling. The most obvious explanation of the difference is that the open-topped shells of the present study are *statically determinate*, whereas the usual closed-ended shells of tests reported in the literature are *statically indeterminate*; the possibility of high initial stresses may explain the scatter in the experimental observations in the literature.

Keywords: Cylindrical shell structures; Self-weight buckling; Classical buckling theory; Non-linear buckling; Finite-element method; Post-buckling; Static determinacy; Initial imperfection; Initial stress

1. Introduction

Thin-walled shells are, in general, highly efficient structures; and they have wide practical application, for example, in the aerospace, petrochemical and construction industries. When thin-walled shell structures are loaded in compression, their strength is limited by buckling; and since such buckling is

* Corresponding author. Tel.: +44-01223-332725; fax: +44-01223-332662.
E-mail address: crc@eng.cam.ac.uk (C.R. Calladine).
[1] Present address: Civil and Structural Engineering Department, UMIST, P.O. Box 88, Manchester, M60 1QD.

0020-7683/00/$ - see front matter
PII: S0020-7683(99)00160-2

Nomenclature

g	acceleration due to gravity
n	number of circumferential waves
t	thickness of shell
w	radial component of displacement
z	height co-ordinate of shell
E	Young's modulus of elasticity of material
L	height of shell
L_{cr}	critical height of shell
R	radius of shell
T	thickness of beam
δ	deflection of cantilever beam
θ	angular co-ordinate
λ	projecting free length of cantilever beam
ν	Poisson's ratio of material
ρ	mass density of material
σ_{cr}	critical compressive stress of cylindrical shell

often catastrophic, reliable prediction of the buckling strength of shells is a strong aspiration of engineers. The present paper is concerned with aspects of the elastic buckling of thin cylindrical shells under axial compression.

Euler's pioneering investigation (1744) of the elastic stability of slender columns paved the way for the development of the 'classical' theory of elastic buckling of structures, in which the governing equations of the problem are linearised, and the resulting eigenvalue problem yields the bifurcation buckling loads as eigenvalues, and the corresponding modes as eigenvectors. That kind of theory has wide application (e.g., Timoshenko and Gere, 1961), and it was applied to the buckling of cylindrical shells between 1911 and 1934 by many independent workers, including Lorenz, Southwell, von Mises, Flügge, Schwerin, Donnell (for a full count see Timoshenko and Gere, 1961, Chapter 11; Brush and Almroth, 1975, Section 5.1). Classical theory predicts that cylindrical shells buckle under uniform axial compressive stress σ_{cr}, given by

$$\sigma_{cr} = \frac{E}{\sqrt{3(1-\nu^2)}}\left(\frac{t}{R}\right) \tag{1}$$

where E is the Young's modulus of elasticity and ν the Poisson's ratio of the isotropic material, t is the wall thickness and R is the radius of the shell.

Experimental studies in the 1930s in connection with aircraft construction (see Fig. 1) revealed that

(a) experimental buckling loads were often much below the predictions of classical theory;
(b) there was a wide scatter in buckling loads for nominally identical specimens; and
(c) the failures were often catastrophic.

These disturbing facts, which were confirmed in many experimental investigations (see Brush and Almroth, 1975) have attracted the attention of many researchers ever since. An early breakthrough in understanding of these paradoxical buckling observations was achieved by von Kármán et al. (1940) and von Kármán and Tsien (1941). They argued that the behaviour of a cylindrical shell under axial

compression is essentially non-linear, and there is a sharp decrease in load-carrying capacity after the peak value of load has been reached. They were able to simulate the main features of shell buckling by means of experiments on a simple model column that was laterally restrained by a slightly non-linear spring that represented the 'stretching' behaviour of the shell; see Calladine (1983) for a modern account. Not long afterwards Koiter (1945) developed a general non-linear theory of elastic stability, which is capable of determining the stability of equilibrium at or near the bifurcation buckling point. He found that cylindrical shells under axial compression exhibit unstable postbuckling, and that the maximum load-carrying capacity is influenced by the presence of initial geometric imperfections: a small imperfection disproportionately reduces the buckling load. These concepts of 'non-linearity' and 'imperfection-sensitivity' go some way towards providing an explanation for the shell-buckling paradox. However, extensive studies based on precise measurements of geometrical imperfection in physical shells, manufactured in various ways, have had less than complete success in predicting buckling load: see Arbocz and Babcock (1969), Arbocz (1974) and Arbocz and Hol (1991). Therefore, it is reasonable to claim that there must be some crucial factors involved in the mechanisms of shell buckling which have been missing hitherto from analytical investigations.

The present paper reports on simple experiments on the self-weight buckling of some small-scale, thin, open-top, fixed-base silicone rubber cylindrical shells. The shells with the highest value of t/R buckled at almost the heights predicted by the 'simple classical theory'. But in general the buckling heights were found to be proportional to $(t/R)^{1.5}$, compared to $(t/R)^{1.0}$ as in the classical theory. Moreover, the

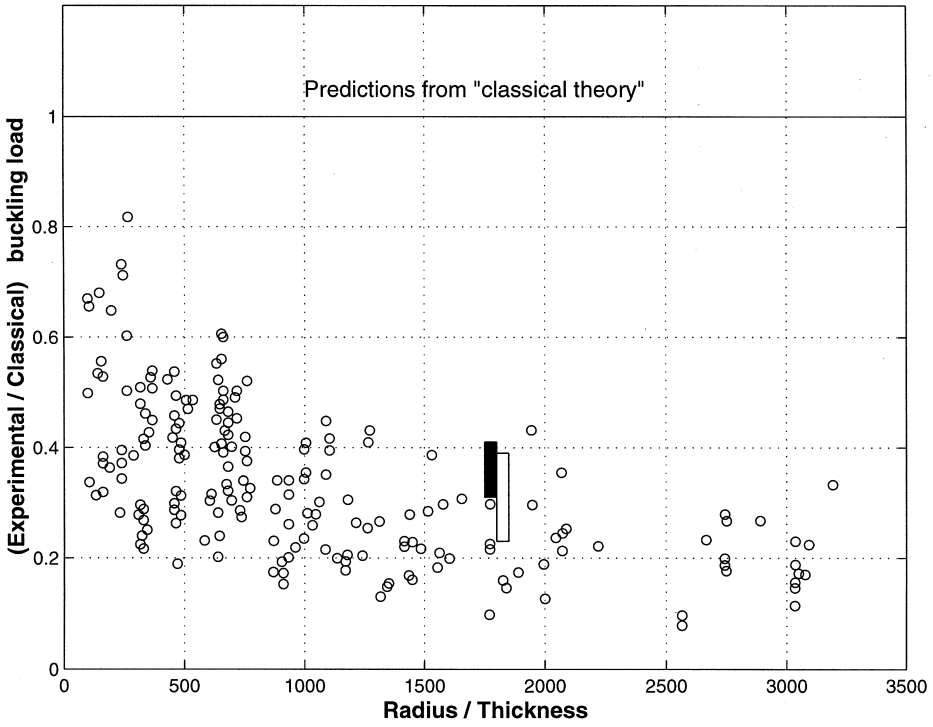

Fig. 1. Distribution of buckling test data for cylinders with closed ends subjected to axial compression, from Brush and Almroth (1975), and supplemented (see Section 6) by ranges of data from Lancaster et al. (1999) on a particular cylinder without (solid bar) and with (open bar) deliberately introduced imperfections. The data are normalised to the predictions of the classical theory of buckling, Eq (1).

buckling heights showed very little 'scatter', although there was no conscious attempt to manufacture very accurate shells; and indeed, there were measurable imperfections in terms of thickness variations. These observations thus defy somehow the widely accepted hypothesis of 'imperfection-sensitivity'. Some non-linear finite-element computations shed an interesting light on these observations.

2. Experiments on self-weight buckling

Several years ago, Calladine and Barber (1970) conducted some experiments on the self-weight buckling of thin cylindrical shells. They manufactured a series of small-scale, open-top, fixed-base, thin cylindrical shells in silicone rubber. The specimens were cast in a specially made rotating mould, that will be described below. The cylinders were cut down, little by little, until they could just be made to stand upright under their own weight (details will be given below). These heights were regarded as the *buckling heights* under self-weight. All of the cylinders had the same outside diameter (nominally 172 mm) and ranged in thickness from 0.23 to 1.12 mm. Altogether there were seven specimens with thickness variations within ± 0.025 mm, and with radius-to-thickness ratio varying from about 80 to 400.

These workers found that the thicker and taller cylinders collapsed in a crumpling mode initiating at the base, like the falling of a heavy curtain; but the thinner cylinders collapsed from the top, like a wall falling inward. In the absence of a suitable theoretical analysis, the results were compared with the classical value of critical compressive stress (1) for a weightless uniform elastic cylindrical shell compressed between its ends. Thus, the simple assumption was made that self-weight buckling would occur when the compressive stress at its base due to dead weight reached the classical critical stress. The critical height (L_{cr}) of the cylinder could thus be expressed, according to this *simple classical theory* as

$$\frac{L_{cr}\rho g}{E} = \frac{1}{\sqrt{3(1-\nu^2)}}\left(\frac{t}{R}\right) \tag{2}$$

where ρg is the weight per unit volume of material. (More thorough versions of the classical analysis will be described in Section 3 below.)

The experimental results are plotted in a dimensionless form in Fig. 2. There are two distinguishing features of these results. First, in general the buckling clearly does not take place according to the 'simple classical theory'. Second, there is very little scatter, compared to almost all buckling tests on thin cylinders that have been reported in the literature (see Figs. 1 and 3). The best-fit line through these experimental results (Fig. 2) can be expressed as

$$\frac{L_{cr}\rho g}{E} \propto \left(\frac{t}{R}\right)^{1.5}, \quad 80 < R/t < 400. \tag{3}$$

Note that the thickest cylinder happened to buckle at almost exactly the value given by the classical analysis (2). That particular cylinder was almost as long as the mould; and so it was not practicable to investigate thicker specimens.

In the experiments of Calladine and Barber (1970), which we shall refer to henceforth as 'the previous experimental study', all of the specimens had the same external diameter. Therefore, notwithstanding the fact that the experimental results were analysed in dimensionless form (Fig. 2), there is a lingering worry that the results — perhaps on account of unavoidable imperfections — might have turned out differently if the diameter, as well as the thickness, had been varied. It was for this reason that the present series of specimens was made with a different mould, of larger diameter.

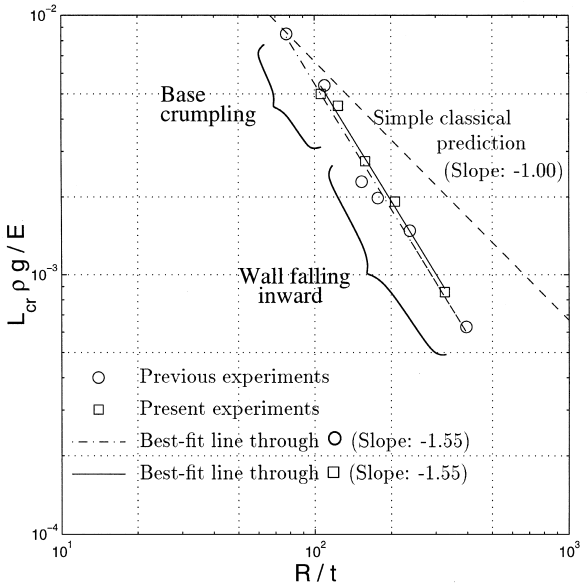

Fig. 2. Experimental results of self-weight buckling height of cylindrical shells.

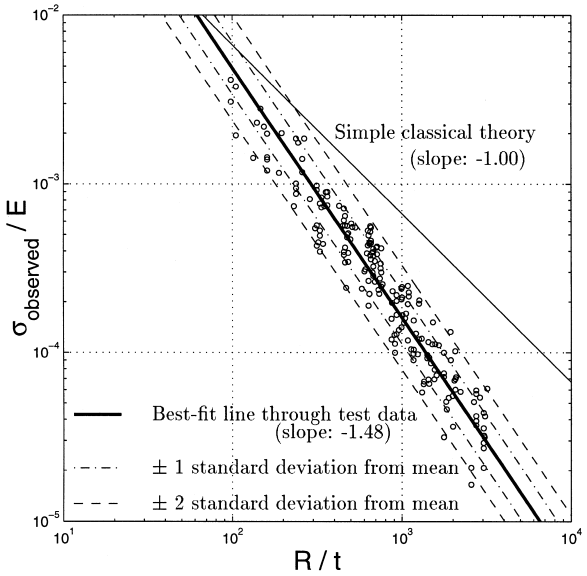

Fig. 3. Distribution of buckling test data for cylinders subjected to axial compression; data from Brush and Almroth (1975), as in Fig. 1 but replotted on log scales.

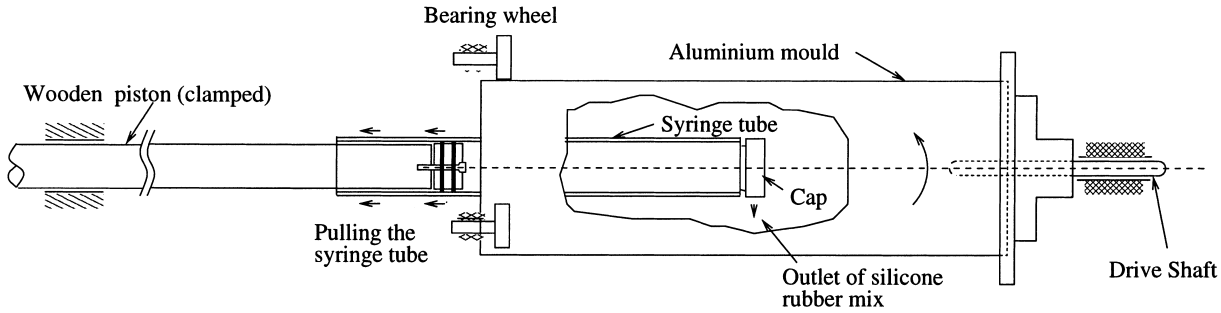

Fig. 4. Manufacturing details for silicone rubber shells (schematic).

2.1. Manufacture of the shell specimens

The cylinders were cast in a horizontal rotating cylindrical mould, with an open end, as shown schematically in Fig. 4. The apparatus was a re-build of Barber's, but with a mould of 40% larger diameter. The mould was turned by an electric motor through a variable-speed drive. Silicone rubber solution (ICI Silcoset 105; ICI Silicones F111/5000, 10% by volume; and Curing Agent A, 1% by volume) was first de-aerated and then deposited inside the mould, revolving slowly at approximately 10–15 rpm, by a specially manufactured set of long syringes. Thus, the piston was held against a fixed stop and the barrel of the syringe was withdrawn slowly and steadily, by hand; a spiral thread of rubber solution was thus deposited uniformly over the inside of the mould. When the desired quantity of rubber solution had been introduced, the mould was rotated rapidly at approximately 600 rpm for a few minutes, until the solution had spread uniformly. This was followed by rotation between four and five hours at the lower speed. When the rubber had hardened, and usually the day after casting, the mould was detached from its bearings, stood upright on a horizontal flat surface, and a quantity of rubber solution was carefully poured inside in order to cast a solid base about 15 mm thick. When this base had hardened, the entire cylinder was carefully removed from the mould.

In total, five new cylinders were cast. The outer diameter of all the cylinders was 241 mm. Thicknesses were chosen in order to keep the ratio R/t within the range investigated previously. Three of the specimens were made by using a single syringe of internal diameter 9.5 mm, filled once, twice and three times, respectively. Intermediate thickness were achieved by using that syringe together with one of diameter 7 mm, which had approximately half the capacity. In Table 1 the specimens are numbered in chronological order of casting, but are listed according to their R/t values.

The standard deviations of thickness given in Table 1 are based on independent measurements of thickness at about 36 points on a regular grid extending over the surface of each shell, with 6 points

Table 1
Geometry of the manufactured cylindrical shell specimens

Specimen	Average thickness (mm)	Standard deviation of thickness (mm)	Outside diameter (mm)	Mean diameter (mm)	R/t
Cylinder 1	1.13	0.032	241	240	106
Cylinder 5	0.97	0.022	241	240	124
Cylinder 2	0.76	0.012	241	241	158
Cylinder 4	0.58	0.016	241	241	208
Cylinder 3	0.37	0.012	241	241	326

around the circumference and about 6 along the length. In general, the standard deviation of thickness is about 3% of the mean thickness.

A careful survey of the geometry of the interior surface of the mould revealed that the radius had a measurable component proportional to $\cos 3\theta$, where θ is a circumferential angular co-ordinate, with amplitude about 0.5 mm, roughly constant along the length of the mould. We were apprehensive that, if the inner surface of the fluid contained in the rotating mould had been truly circular, there would have been a systematic component of the same type in the thickness of the shells. However, thorough measurements revealed that there was hardly any effect of this kind; evidently, the transport of fluid silicone rubber over the surface during high-speed spinning operated well over lengths of the order of the spacing of the silicone rubber 'threads' as deposited, but not over larger lengths.

2.2. Measurement of $E/\rho g$

The plot of Fig. 2 incorporates the measured critical height L_{cr} into the dimensionless group $L_{\mathrm{cr}}\rho g/E$ by dividing by the single material parameter $E/\rho g$, which has the dimension of length. In order to measure the value of this parameter, a slender rectangular beam of thickness T was cast from the same batch of material from which each cylinder had been cast. Fixing this specimen as a cantilever beam at one end between two heavy metal blocks, the projecting free length λ was adjusted so that the cantilever, after deflecting under its own weight, just touched the base. In other words, the height of the lower clamping block δ was the self-weight deflection of a cantilever beam of length λ. The process was repeated, using blocks of different height. In this way, a set of data was obtained for the length λ of the beam and the corresponding self-weight deflections at its tip. Assuming small-deflection theory is appropriate, the value of $E/\rho g$ can be obtained as

$$\frac{E}{\rho g} = \frac{1.5}{T^2}\frac{\lambda^4}{\delta} \tag{4}$$

Applying this equation, we can estimate the value of $E/\rho g$ by plotting λ^4 against δ. In practice, these points lie on a good straight line for any given specimen. The average value of E/ρg for the five specimens was 118 m. The variation from specimen to specimen is shown in Table 2. The density of the cured silicone rubber was found to be 1200 kg/m^3.

2.3. Measurement of critical buckling height, L_{cr}

When a specimen had been extracted from the mould and placed on a flat, horizontal table, attempts could be made to stand the cylinder upright. In order to determine whether or not a cylinder of given height can stand on its own under gravity, it is necessary first to hold the floppy specimen in a properly cylindrical shape. Then, if it fails to stand when released, say after five or six attempts, its current length

Table 2
Buckling height of cylinders

Specimen	Average thickness (mm)	$E/\rho g$ (m)	L_{cr} (mm)	R/t	Mode
Cylinder 1	1.13	119	595	106	Base crumpling
Cylinder 5	0.97	114	512	124	Base crumpling
Cylinder 2	0.76	120	331	158	Wall falling inward
Cylinder 4	0.58	120	230	208	Wall falling inward
Cylinder 3	0.37	117	100	326	Wall falling inward

is larger than L_{cr}, and it must be shortened in readiness for another attempt. In the previous experimental study, Barber found that the diameter of his specimens was such that he could support them temporarily by using the fingers of both hands. The new cylinders of the present series were of larger diameter; and so a manual scheme of temporary support would require more hands. We investigated the use of a simple mechanical device for erecting the cylinders, consisting of an interior tube which fitted loosely, and which could be hoisted vertically out of the top, to leave the thin rubber cylinder standing, or otherwise. Although such a scheme could probably have been made to work, it would have required precision manufacture and operation. In the meantime we discovered that, with experience, the manual scheme worked well.

It is not easy to describe the process of manual erection of a floppy cylinder, because it involves an acquired hand/eye co-ordination on the part of the people involved. The main objective is to get the silicone rubber shell, particularly at the top, to take a truly cylindrical form. Any portion which tends to fall inwards must be caught and restrained. The thumb and finger of one hand can be used to provide a gentle restraint, and to pull upwards or push circumferentially in order to control a potential collapse. Usually, three or four people held the top of the open cylinder, before slowly releasing their grip. The shape of the cylinders just before release was doubtless not perfectly circular; probably there were radial displacements at the top of the order of ± 1 mm. All of the cylinders were cast longer than the buckling length predicted by simple classical theory. Consequently, at the first attempt to stand any of the cylinders upright, it always collapsed. Next the cylinder was cut down by a small amount, usually in the range 5–10 mm. At each new height, five or six trials were given with great patience, almost holding one's breath. If the specimen still would not stand, the process was continued until the rubber cylinder did just stand upright under its own weight. This height (above the base) was measured and was recorded as the self-weight buckling height, L_{cr}. When the gradually reducing height of a specimen approached the height interpolated from the results of the previous study, the slices cut-off were restricted to a maximum of 5 mm. Therefore, we can accept the measured buckling heights L_{cr} with confidence to within 5 mm.

2.4. Observations

The modes of collapse were the same as those observed in the previous study. Thus, the thicker cylinders (Cylinders 1 and 5) collapsed in a crumpling mode initiating at the base; but the thinner cylinders (2, 3 and 4) collapsed like a wall falling inward. Such collapses occurred at random locations around the circumference. The critical heights are plotted in Fig. 2, alongside those of the previous study. The best-fitting straight lines through the two sets of points (as determined by a regression algorithm) are found to have almost identical slopes, but the line for the new data is higher by 3%. This possibly reflects the greater care used in the present tests to determine the critical heights. The standard deviation of the experimental points corresponds to 6% of the measured height for the new data, in comparison with 13% for the previous study.

3. Classical analysis

As mentioned in Section 1, the usual explanation for low experimental buckling loads in relation to the predictions of classical theory is that thin cylindrical shells are highly imperfection sensitive, and small initial imperfections are unavoidable; thus, the random nature of these unavoidable small imperfections causes scatter in the experimental data. However, the level of scatter in the present and

the previous experiments on self-weight buckling is very small. A possible explanation if this feature of the observations might, therefore, be that the buckling is indeed of a classical kind; and that the discrepancy between the observations and the simple classical theory might just be that the theory is *too* simple. Let us, therefore, re-examine the theory as described above in Section 2.

Weingarten (1962) investigated the effect of linearly varying axial compressive stress on the buckling characteristics of circular cylindrical shells simply-supported at both ends. The calculation was done according to the classical theory. He found that the maximum critical compressive stress induced by longitudinally varying axial load (such as self-weight loading, where the stress level increases towards the bottom of the shell) was in general higher than the critical uniform compressive stress corresponding to loading applied only at the ends of the shell. The results from his calculations suggest that the simply-supported circular-cylindrical shell under self-weight loading buckles when the compressive stress *at one classical axial half-wave-length from the bottom* reaches the buckling stress predicted by the classical theory (2). Thus, according to Weingarten's analysis, an *improved classical formula* (to first order) can be written as

$$\left(L - m1.76\sqrt{Rt}\right)\frac{\rho g}{E} = 0.63\frac{t}{R} \tag{5}$$

where $m = 1$, and $1.76\sqrt{Rt}$ is one axial half-wave length. Here, the value of ν has been fixed at 0.3. The upshot of this refinement is thus to increase the value of L_{cr} above that predicted by Eq. (2) by a small amount that increases, in comparison with L_{cr}, as R/t decreases. Hence, Weingarten's analysis tends to increase L_{cr} over the value given by Eq. (2), rather than to decrease it as in the experiments; and while his analysis makes the theoretical curve somewhat steeper than the plot of Eq. (2) in Fig. 2, the overall effect is weak.

The simply-supported end conditions assumed by Weingarten do not, of course, correspond either to the free upper end or to the built-in lower end of our experimental specimens. But a simple linear, eigenvalue analysis by means of the finite-element method (FEM) for Weingarten's situation but with a built-in lower edge again produces formula (5), but with the value of m increased from 1 to 3. A separate analysis of the same kind showed that the buckling load was not affected when a free end-condition was imposed at the top.

Thus, none of the above 'improved' classical analysis can possibly explain the empirical observation that the critical height is proportional to $(t/R)^{1.5}$, other things being equal.

In this connection, it is perhaps worth mentioning that a classical buckling analysis that does indeed involve a buckling load proportional to $(t/R)^{1.5}$ was discovered, almost by accident. The experimentally measured critical heights correspond to a situation in which a cylindrical shell with a fixed base and open top, *but in a gravity-free environment*, is loaded by a uniform radial-inward directed pressure equal to approximately one-tenth of the weight of the shell per unit area. There is a well-known classical analysis for this problem (see Calladine, 1983, Section 14.6 for details and formulas); and in particular it gives a critical height proportional to $(t/R)^{1.5}$, just as in the experiments shown in Fig. 2. The critical mode involves radial displacements which are periodic around the circumference, and which increase steadily from bottom to top. The formulas for critical pressure and circumferential mode-number have been confirmed by an ABAQUS linear-eigenvalue analysis for a few cases. There is, however, no rational connection between a gravity-free pressure loading on the one hand, and the actual self-weight loading under investigation on the other; and, therefore, this appearance of a $(t/R)^{1.5}$ term cannot be directly relevant to the present problem. The only useful feature of this particular piece of analysis is the mode-form, which will be borrowed, in an adapted version, for use in Section 5; and it will appear in the post-buckling behaviour of the shell.

4. Comparison with other experimental data

Experimental data on the buckling loads of axially end-loaded cylindrical shells from various sources have already been displayed in Figs. 1 and 3 in order to demonstrate the wide scatter in buckling loads that is commonly found in such testing. Two points emerge clearly from the plot of Fig. 3.

First, the slope of the best-fit line is very close to -1.5; and indeed the best-fit line itself is close to that obtained in the present experimental programme; compare Figs. 2 and 3. Second, the observed scatter in buckling load is uniform for a wide range of R/t values; practically, all the data lie within a factor of 0.6–1.6 with respect to the best-fit line — corresponding to ± 2 standard deviations. One standard deviation corresponds to a factor of 1.3 on load; which is much larger than the standard deviations measured in the present and previous self-weight buckling assays (Section 2.4).

Finally, it may be mentioned that von Kármán et al. (1940) in their seminal paper on shell buckling also commented that the then available experimental buckling loads were proportional to $(t/R)^{1.4}$, instead of $(t/R)^{1.0}$ as predicted by classical theory.

5. Non-linear FEM analysis

It is clear from Section 3 that there is no way by which classical buckling analysis can explain the self-weight buckling behaviour as observed in the present and the previous experimental studies. The lack of 'scatter' in the observations, which seemed, misleadingly, to suggest a classical approach, must be attributed to some other factor.

It is, therefore, necessary to consider seriously non-linear behaviour; and the most convenient way of doing that is to use the FEM. The well-tried ABAQUS non-linear package was available.

In the non-linear FEM analysis, all shells were taken to have uniform thickness. Element size and type were chosen by conducting first the linear, eigenvalue analyses already mentioned (see Mandal, 1997). Only geometric non-linearity has been considered; the silicone rubber material of the cylinders may be taken as linear-elastic for all practical purposes. ABAQUS uses the modified Riks method to solve any general non-linear problem. The method is particularly suitable for obtaining non-linear static equilibrium solutions for unstable problems, where the load and/or the displacement may decrease as the solution evolves.

The buckling loads of axially compressed thin cylindrical shells are extremely sensitive to the presence of initial geometric imperfections, at least according to the received view. A non-linear analysis can be conducted for large deflections provided there is proper modelling of initial geometric imperfections. An important problem, therefore, lies in the choice of the amount and nature of the assumed imperfection. Now, Koiter's early non-linear studies (Koiter, 1945) demonstrated that an initial geometrical imperfection in the form of a classical eigenvector mode could have a big impact on the subsequent behaviour. Hence, one way of proceeding in the present case would be to do first an eigenvalue analysis of a perfect structure, and then to use the first buckling mode from that analysis as a trial imperfection. The magnitude of imperfection could then be found out by interpolation on the basis of existing experimental results. Such a method is appealing to designers. However, in the present study, where it is aimed to resolve the paradox of self-weight buckling height varying in proportion to $(t/R)^{1.5}$ and with very little scatter, there is need for a different approach.

Visual observations of self-weight buckling of the thinner-walled open-top cylindrical shells suggest that a circumferentially localised radial-inward displacement mode is a frequent feature of the actual 'falling wall' collapse mechanism. It seemed desirable, therefore, to introduce an initial imperfection of the same general kind into the shell. Although no direct connection could be made (see Section 3) between the classical buckling of an open-top cylindrical shell under external pressure (but without

gravity) and the buckling of a vertical shell under gravity, the buckling mode of the shell under external pressure suggested a form of imperfection that might be worth trying. Thus, an imperfection of the form

$$w = w_0\left(\frac{z}{L}\right)\cos n\theta \tag{6}$$

where z is a height co-ordinate with origin at the base, θ is a circumferential angular co-ordinate, and n is given by classical analysis of buckling under radial-inward pressure, was used, at various amplitudes, as a starting imperfection on a shell having the leading dimensions of one of the experimental specimens, Cylinder 4.

The shell was set up with such an imperfection, and a computation was performed with steadily increasing gravity as the loading parameter. Unfortunately, no useful patterns of behaviour emerged as the load was increased. There seemed to be no distinctive feature around the circumference from which a particular, localised, buckle — as in the experiments — might form. Accordingly, a variant of this mode-form was tried instead, in which a localised inward initial displacement was introduced by multiplying the previous mode (6) by a function, $\mathrm{e}^{-k\theta^2}$, which decayed strongly in the circumferential direction:

$$w = w_0\left(\frac{z}{L}\right)\cos(n\theta)\mathrm{e}^{-k\theta^2}. \tag{7}$$

Here, w_0 is the maximum amplitude of imperfection, usually expressed as a fraction of the thickness of the cylinder. For Cylinder 4, $n = 7$. The constant k was selected so that the amplitude of the radial displacement at $\theta = \pi/7$ (i.e., at one half-wave from the centre of the pattern) was 0.25 of the amplitude of displacement at $\theta = 0$.

Taking the imperfection as in Eq. (7), and the maximum amplitude as one fourth of the thickness and pointing inwards (i.e., $w_0 = -0.25t$) a non-linear analysis was performed, under varying load. This kind of computation showed some interesting features. The radial displacements at three particular points on the surface of the shell are plotted against the gravity load factor in Fig. 5(a). Node 741 is at the top, on the plane of mirror-symmetry, where the amplitude of initial imperfection is maximum; while node 748 is one half-wave of the initial waveform around the circumference. The displacements at these two points came out to be proportional to each other at all stages, displacements at node 748 in general being approximately $-\frac{2}{3}$ of those at node 741. Of perhaps more interest is the displacement at node 260, which is near the bottom of the shell and on the plane of symmetry. As node 741 moves out, node 260 moves in; and at all stages the magnitudes of the two displacements are approximately equal. Node 260 was selected for plotting because it had the largest inward radial displacements in the early development of buckles.

The cylinder shows practically axisymmetric behaviour up to the point of maximum load. This maximum load is only 10% below the classical buckling load, as calculated by linear eigenvalue FEM analysis. The axisymmetric pre-buckling behaviour corresponds broadly to that which was found in Weingarten's (1962) analysis. Thus, at a given value of gravity, the compressive stress due to self-weight is proportional to distance from the top of the shell; and there is a corresponding 'Poisson' radial expansion. But this is prevented at the fixed base; and so an axisymmetric 'bulge' forms near the base, with maximum radial outwards displacement one half-wavelength up from the base — where a half-wavelength is approximately equal to the classical 'beam-on-elastic-foundation' value of $1.76\sqrt{Rt}$. Half a wavelength higher than that, there is a maximum inwards radial displacement, relative to the simple 'Poisson' expansion; and here, therefore, is a band of hoop-wise compression. This band of circumferential compression, in conjunction with the vertical, axial self-weight compression, predisposes

the shell to buckle by bifurcation locally in a periodic mode around the circumference, in broadly the way explained by Koiter (1963, 1978) in a somewhat similar situation.

After the maximum load has been reached, the shell starts to deform in a non-symmetric mode, and the load decreases sharply as deflections increase. With this reduction in load, an isolated dimple forms near node 260 (see Fig. 6(a)), within the axisymmetric 'ring' of circumferential compression which was formed, as explained above, at the maximum load. As the load falls from its peak value, the

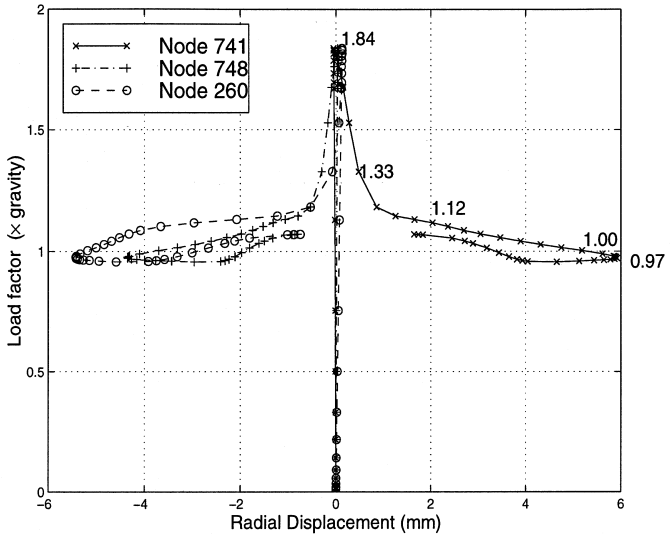

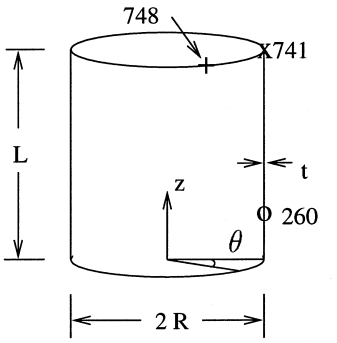

Imperfection:

$$-0.25\,t\,(z/L)\,\cos(7\theta)\,e^{-6.9\,\theta^2}$$

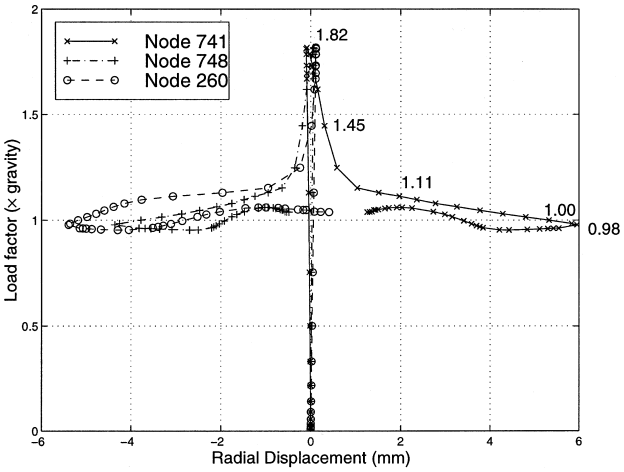

(b)

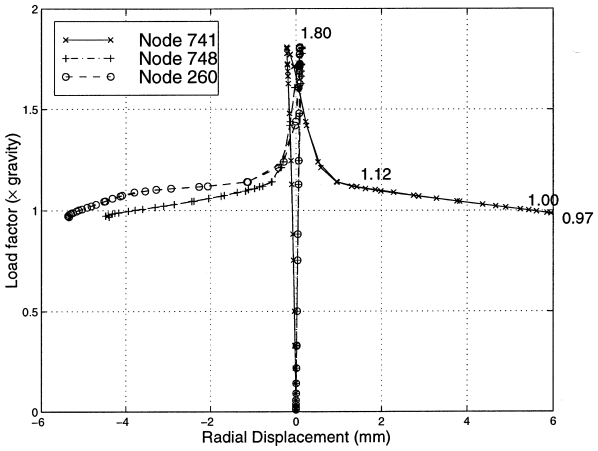

(c)

Fig. 5. Non-linear analysis under vertical gravity for Cylinder 4 ($t = 0.58$ mm, $L_{cr} = 230$ mm and $L = 230$ mm). The location of three particular nodes is shown on the right of (a). Imperfection amplitude: (a) $-0.25t$, (b) $-0.50t$, and (c) $-1.00t$. Numbers shown against some points on the curves indicate load factor values.

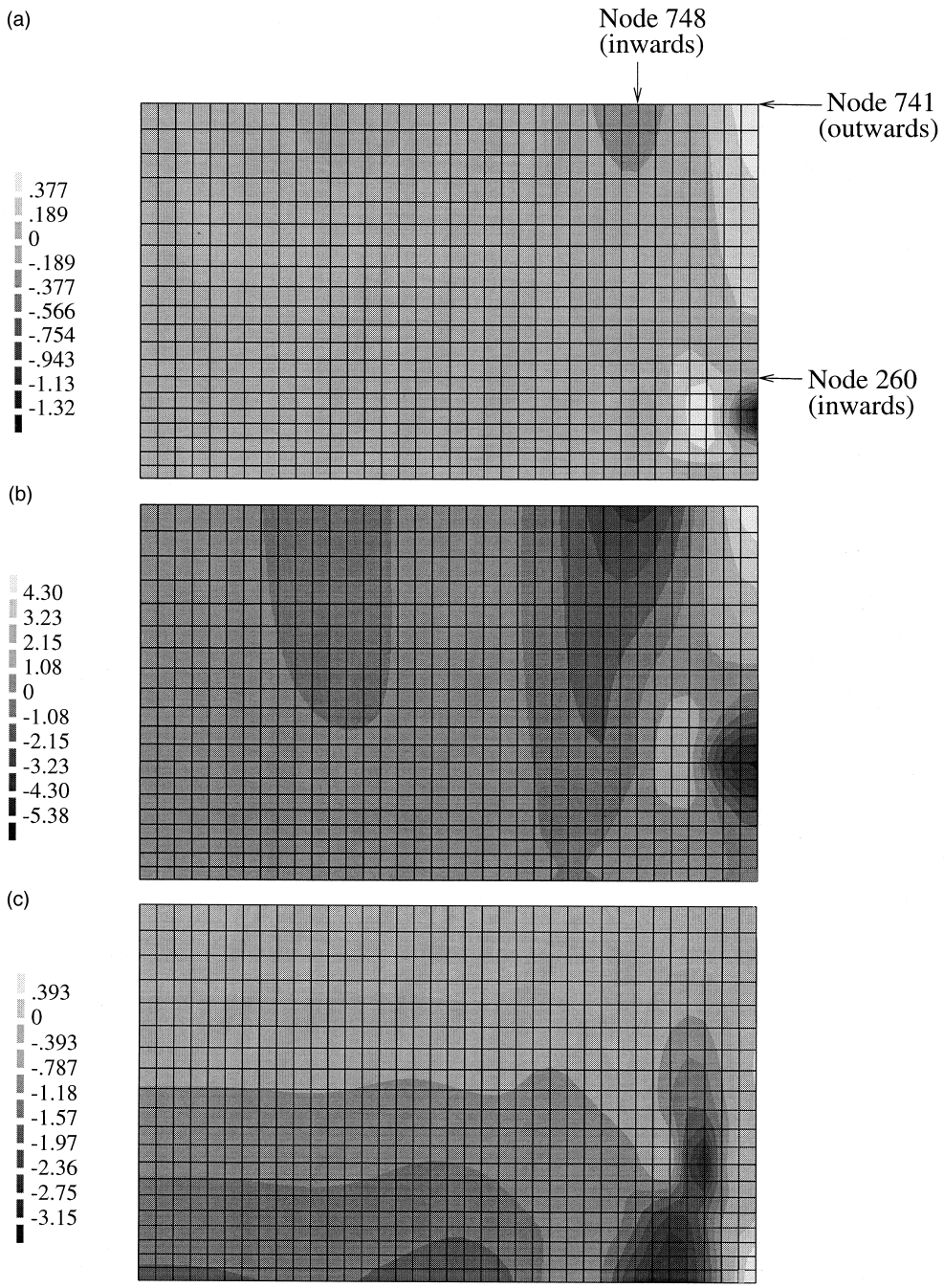

Fig. 6. (a) and (b) Contour plot of radial displacement (mm) in Cylinder 4 (see Fig. 5) for load factor: (a) 1.33 g, (b) 1.00 g. Half of the cylinder has been unwrapped, with the initial imperfection at the right, and with the opposite diameter on the left. The three nodes shown in Fig. 5(a) are identified in (a). The non-uniform grid was used for all computations. Positive displacements (light tone) are outwards. (c) Contour plot of axial membrane force (N/m) for load factor 1.00 g, and with a radial displacement of approximately 6 mm at Node 741 (see Fig. 5(a)).

axisymmetric rings disappear but the remaining isolated dimple seen in Fig. 6(a) grows in size, as in Fig. 6(b), with its radial (inwards) displacement always approximately equal to the radial (outwards) displacement at the top of the shell (node 741), as already mentioned.

But the most striking result of these computations is that the load-displacement curve exhibits a flat-plateau near unit gravity; the load remains practically constant while the radial displacement increases to about ten shell thicknesses. To the best of our knowledge, this is qualitatively unlike anything seen in previous non-linear computations of shell buckling. In the sense that this 'robust' plateau occurs at unit gravity in a shell having the experimentally observed critical height, this behaviour seems to support the experimental findings. However, on further pursuing the load-deflection equilibrium path, the dimple starts to migrate upwards, and hence the load-path takes again an upward journey.

Now if the initial imperfection (7) were simply to grow in amplitude in a more-or-less inextensional way, it would require some small vertical downwards displacement at the bottom of the shell. Such a displacement is prevented, of course, by the 'clamped' boundary conditions there. However, the localised dimple near node 260 appears effectively to perform the function of allowing the small vertical displacements that are required by the almost-inextensional displacement of the upper part of the shell.

A close examination of the well-established dimple showed that there is high axial compressive membrane stress at the edges of the dimple, while it is low at the centre. Fig. 6(c) shows the contour plot of axial membrane force N_x at unit gravity. And it can be observed that directly under the dimple there is a *tensile* axial force near the base. Therefore, at this stage the dimple zone is not supporting at all the weight of the cylinder. Another computational study has been conducted with a portion of the base of the shell cut out, so that it cannot support the compressive load directly. The point of those calculations was to investigate whether the inward-dimple at the base could be represented, in a first approximation, by a simple cut-out, in view of the remarks made above. The stress distribution in the presence of this sort of cut-out was specially interesting; but the study was inconclusive in the sense that the cut-out did not directly mimic the effect of the dimple as found in the full computation; it was evidently too crude a model.

Next, in order to study the imperfection sensitivity of the buckling, the amplitude of the same kind of imperfection was altered, and the program re-run. Fig. 5(b) and (c) show plots of load factor versus radial displacement of the same cylinder, but with imperfections having amplitude twice and four times the imperfection used for Fig. 5(a). From these plots it is seen, surprisingly, that the amplitude of the initial imperfection makes almost no difference to the overall behaviour; both the initial buckling load and the well-defined post-buckling plateau are practically unaltered by the four-fold change in amplitude of the initial geometric imperfection.

Moreover, it was found that the same flat plateau was present even when the *direction* of the imperfection was reversed, i.e., when the initial displacement was outward at the plane of symmetry; and indeed a similar flat plateau was found when corresponding analyses were made of Specimens 2 and 5.

The existence of a 'post-buckling plateau' at almost exactly the experimental buckling load strongly suggests an explanation for the observed buckling behaviour of the shell. It seems that there is a post-buckling mode which is reached, at least in the FEM calculation, only after access to it has been gained at a rather high initial load. It is clear from the computations that initial buckling is *not* sensitive to the amplitude of the imperfection mode-form that has been assumed. But it seems plausible that some other initial mode-form — as yet unknown, but possibly related to the presence of the many fingers in the experiments as described in Section 2.3 — could give access to the special post-buckling mode *without* the need to overcome a high initial load barrier. Somehow, it seems that it is the very well-defined 'post-buckling-plateau' load that dominates the experimental behaviour. The surprising constancy of the post-buckled-plateau load as the deflection increases — which we repeat has not, so far as is known, been observed before — suggests that there might be some 'almost classical' analysis that would describe this strange feature of the non-linear behaviour of the shell. Such an analysis would not be truly classical, of

course; otherwise it would have been found by the linearised analysis reported in Section 3. Nevertheless, there might well be a way of performing some sort of relatively simple calculation that would convincingly describe the post-buckling-plateau feature.

6. Discussion

The concepts of *non-linearity* and *imperfection-sensitivity* are widely used to explain the low buckling loads and their high scatter in many experimental studies of cylindrical shells. But our experiments on self-weight buckling of thin, open-top, cylindrical shells, on the contrary, exhibited almost negligible scatter, although measurable geometric imperfections were indeed present. Apart from the different levels of scatter, the general trend of our experimental results also fits well with a large quantity of previous experimental data on the buckling of cylindrical shells with closed ends under end-wise axial compression. In both cases, the average critical stress level is proportional to $(t/R)^{1.5}$, compared to $(t/R)^{1.0}$ as in classical theory, Eq. (1).

There is evidence from our FEM analysis that the experimental value of self-weight buckling height could be predicted numerically. The mechanism of initial buckling is still not very clear; the initial buckling load might, of course, be affected by the choice of initial imperfection, both its mode-form and its amplitude. Non-linear analysis carried out with different amplitudes of the same imperfection mode showed, surprisingly, that the peak load was always nearly the same. But at all amplitudes of imperfections, high deflections were observed to occur under unit gravity. The existence of a post-buckling-plateau load in the computations at the experimentally observed load for Cylinders 4, 2 and 5 strongly suggests an explanation for the observed behaviour. In particular, the extreme insensitivity of the 'plateau load' to the amplitude of the initial imperfection suggests an explanation for the absence of scatter in the experimental observations.

In the light of these findings, we suggest that a line of explanation of the striking differences between the present self-weight experiments (Fig. 2) and the collected experimental data from literature (Fig. 3) lies in the fact that the two sets of shells have a different status in terms of *static determinacy*; thus, open-topped shells are *statically determinate*, whereas shells with closed ends are *statically indeterminate*, from the point of view of membrane-stress analysis. The static indeterminacy in a system may be held responsible for any locked-in stress due to lack-of-fit resulting from the manufacturing process. Such unaccounted locked-in-stresses may cause a shell to buckle at a premature load, after reaching the critical stress in a localised area; or in general, they may produce a big statistical variation in buckling loads. A similar phenomenon was pointed out by Affan and Calladine (1989) in the context of buckling of a statically indeterminate double-layer bar-and-joint grid under load; the higher the level of static indeterminacy the lower the buckling load, on account of random imperfections in the lengths of the constituent bar-members.

The same concept of static determinacy in connection with triangulated, pin jointed space-frame may also be applied to a shell structure, where the whole surface can be idealised as an ensemblage of simple, triangular areas (see Calladine, 1983, Section 4.7 for details). Now, a thin shell is often described as being statically determinate as a membrane, since in principle three unknown membrane stress components acting on an arbitrary element can be determined uniquely from the three local equilibrium equations. However, the kinematic constraints imposed by the boundaries are the decisive factor in determining the overall static indeterminacy of a shell. It follows that a cylindrical shell with simple disc end closures that hold the ends circular, but not plane, is statically determinate; and so also is an open-top, fixed-base shell as used in the present experimental study. These shells are capable of remaining in a stress-free state, even if there are small misalignments during manufacture. Due to lack of locked-in

stresses, it may be argued that these statically determinate shells are likely to show little scatter of critical loads in buckling experiments.

In contrast, the cylindrical shells that have been used in most sets of buckling experiments to date have had ends that are 'fixed' in the sense that they are constrained not only to be *circular* but also *plane*. Such shells may well contain substantial locked-in stresses as a result of the manufacturing process; and such initial stresses may in principle have a big effect on buckling loads. Another aspect of this is that the special mode which ABAQUS indicates as corresponding to the post-buckling-plateau clearly involves significant radial displacements at the free edge of the shell.

Careful avoidance of the possibility of locked-in stresses may even improve the performance of a fixed-ended cylinder with respect to buckling. An experimental study by Lancaster et al. (1999) has shown evidence of that. By some special arrangements at the ends, involving the shell being clamped to end-discs by pre-stressed circumferential belts, these workers were able to remove any locked-in stresses in a melinex cylindrical shell (height 710 mm, radius 440 mm and thickness 0.25 mm) before applying axial load. They found that in spite of the initial geometry of the shell being far from perfectly cylindrical, the experimental buckling loads were unusually high, and lay at the upper end of the wide scatter-band of experimental data from the literature (see Fig. 1).

All of this evidence suggests that the boundary conditions in relation to locked-in stresses play a definite role in shell buckling. Shells with highly constrained boundaries are liable to attract stress in the manufacturing processes, and this stress is additional to any superimposed stress due to loading, thereby causing local buckling, leading to collapse. However, if the initial stresses are somehow removed before applying the load, an almost classical behaviour is observed, at least in the sense that there is little scatter in the experimental buckling load. Thus, the present study suggests that the most disturbing fact about shell buckling — the wide-scatter in the experimental data — can be tackled in practice by arranging the shell boundaries so as to prevent the possibility of locked-in stresses. This approach may possibly help designers to establish a more rational design procedure for cylindrical shells, thereby avoiding the need to rely so much on empirically derived 'knock-down' factors.

7. Conclusions

Experiments on self-weight buckling of thin, open-top, fixed-base, small scale cylindrical shells show some interesting behaviour. There is very little scatter in the present experimental results compared to the scatter in buckling data collected from the literature. The buckling heights were found to be proportional to $(t/R)^{1.5}$ compared to $(t/R)^{1.0}$ as in the 'classical theory'. The best-fit line through the vast experimental data in the literature is also shown to have a slope of approximately 1.5.

A non-linear FEM analysis of open-topped cylinders showed that there is a post-buckling-plateau load corresponding to the experimental buckling loads. The static determinacy of the shells in the present experiments seems to be the most obvious explanation for the small scatter in the experimental results.

The findings reported in this paper can be best described as pointing towards a new hypothesis for the buckling of shells under axial compression. A more rigorous explanation of this problem area requires further detailed research, including more experimental and computational studies.

References

Affan, A., Calladine, C.R., 1989. Initial bar tensions in pin-jointed assemblies. International Journal of Space Structures 4, 1–16.

Arbocz, J., 1974. The effect of initial imperfections on shell stability. In: Fung, Y.C., Sechler, E.E. (Eds.), Thin Shell Structures. Prentice-Hall, Englewood Cliffs, N.J, pp. 205–245.

Arbocz, J., Babcock, C.D., 1969. The effect of general imperfections on the buckling of cylindrical shells. Journal of Applied Mechanics, Trans. ASME 36, 28–38.

Arbocz, J., Hol, J.M.A.M., 1991. Collapse of axially compressed cylindrical shells with random imperfections. AIAA Journal 29, 2247–2256.

Brush, D.O., Almroth, B.O., 1975. Buckling of Bars, Plates and Shells. McGraw-Hill, New York.

Calladine, C.R., 1983. Theory of Shell Structures. Cambridge University Press, Cambridge.

Calladine, C.R., Barber, J.N., 1970. Simple experiments on self-weight buckling of open cylindrical shells. Journal of Applied Mechanics, Trans. ASME, 1150–1151.

Euler, L., 1744. Methodus inveniend lineas curvas maxim: minimive proprietate gaudentes (Appendix, de curvis elastics). Marcum Michaelem Bousquet, Lausanne and Geneva.

Koiter, W.T., 1945. On the stability of elastic equilibrium (in Dutch with English summary). Ph.D. thesis, Delft, H J Paris, Amsterdam. English translation, Air Force Flight Dynamics Laboratory Technical Report, AFFDL-TR-70-25, Ohio, February 1970.

Koiter, W.T., 1963. The effect of axisymmetric imperfections on the buckling of cylindrical shells under axial compression. Proceedings of Konninklijke Nederlandse Akademie van wetenschappen 66, 265–279.

Koiter, W.T., 1978. The influence of more-or-less localised short-wave imperfections on the buckling of circular cylindrical shells under axial compression (in a first approximation). In: Complex Analysis and its Applications. Nauka, Moscow, pp. 242–244.

Lancaster, E.R., Calladine, C.R., Palmer, S.C., 1998. Experimental observations on the buckling of a thin cylindrical shell subjected to axial compression. International Journal of Mechanical Sciences, in press.

Mandal, P., 1997. Buckling of thin cylindrical shells under axial compression. Ph.D. thesis, University of Cambridge, Department of Engineering.

Timoshenko, S.P., Gere, J.M., 1961. Theory of elastic stability (2nd Edn). McGraw-Hill, New York.

von Kármán, T., Dunn, L.G., Tsien, H., 1940. The influence of curvature on the buckling characteristics of structures. Journal of the Aeronautical Sciences 7, 276–289.

von Kármán, T., Tsien, H., 1941. The buckling of thin cylindrical shells under axial compression. Journal of the Aeronautical Sciences 8, 303–312.

Weingarten, V.I., 1962. The buckling of cylindrical shells under longitudinally varying loads. Journal of Applied Mechanics, Trans. ASME 29, 81–85.